Photoinduced Volume Change and Energy Storage Associated with the Early Transformations of the Photoactive Yellow Protein from *Ectothiorhodospira halophila*

Marion E. van Brederode,* Thomas Gensch,‡ Wouter D. Hoff,* Klaas J. Hellingwerf,* and Silvia E. Braslavsky‡

*Department of Microbiology, E. C. Slater Institute, Biocentrum, University of Amsterdam, 1018 WS Amsterdam, The Netherlands, and ‡Max-Planck-Institut für Strahlenchemie, D-45413 Mülheim an der Ruhr, Germany

ABSTRACT   The photocycle of the photoactive yellow protein (PYP) isolated from *Ectothiorhodospira halophila* was analyzed by flash photolysis with absorption detection at low excitation photon densities and by temperature-dependent laser-induced optoacoustic spectroscopy (LIOAS). The quantum yield for the bleaching recovery of PYP, assumed to be identical to that for the phototransformation of PYP (pG), to the red-shifted intermediate, pR, was $\Phi_R = 0.35 \pm 0.05$, much lower than the value of 0.64 reported in the literature. With this value and the LIOAS data, an energy content for pR of 120 kJ/mol was obtained, ~50% lower than for excited pG. Concomitant with the photochemical process, a volume contraction of 14 ml/photoconverted mol was observed, comparable with the contraction (11 ml/mol) determined for the bacteriorhodopsin monomer. The contraction in both cases is interpreted to arise from a protein reorganization around a phototransformed chromophore with a dipole moment different from that of the initial state. The deviations from linearity of the LIOAS data at photon densities >0.3 photons per molecule are explained by absorption by pG and pR during the laser pulse duration (i.e., a four-level system, pG, pR, and their respective excited states). The data can be fitted either by a simple saturation process or by a photochromic equilibrium between pG and pR, similar to that established between the parent chromoprotein and the first intermediate(s) in other biological photoreceptors. This nonlinearity has important consequences for the interpretation of the data obtained from in vitro studies with powerful lasers.

INTRODUCTION

The nature of the chromophore-protein interactions in biological photoreceptors is of major importance as it is strongly linked to the particular function of each photoreceptor. Our own studies of the photoinduced processes of the plant photoreceptor phytochrome (Braslavsky, 1990; Hill et al., 1994; Lindemann et al., 1993; Schaffner et al., 1990) and those from other laboratories (see, e.g., Li and Lagarias, 1992; Rüdiger, 1992; Song, 1988) and studies of the halobacterial membrane protein bacteriorhodopsin (Rohr et al., 1992; Schulenberg et al., 1994), as well as of chromophore-model compounds (Braslavsky et al., 1983), revealed new aspects in this area. The study of the time-resolved protein movements during the photoinduced reaction by using photothermal methods offers an alternative to optical detection to answer some poorly understood mechanisms. This approach has been pioneered by Callis et al. (1972) and applied by Parson's research group to various biological photoreceptor systems (Arata and Parson, 1981; Ort and Parson, 1978).

Essentially, the method is based on the fact that, after pulse excitation, a volume change takes place in the medium. This volume change may be composed of two terms: 1) the expansion or contraction due to the release of heat by radiationless processes from the excited molecules and 2) the pos-

sible volume change due to photoinduced movements concomitant with the photoreaction. While the first contribution is temperature dependent, the second generally is not. Thus, both contributions can be separated by temperature-dependent measurements (Callis et al., 1972; Norris and Peters, 1993; Peters et al., 1992). The volume change may be detected by a rapid pressure transducer and in this case we called the method laser-induced optoacoustic spectroscopy (LIOAS) (Braslavsky and Heibel, 1992).

Using LIOAS, we have determined the energy stored by the microsecond intermediates in the bacteriorhodopsin photocycle (Rohr et al., 1992). More recently, through the temperature dependence of the LIOAS signals from bacteriorhodopsin, we derived the volume changes due to molecular movements taking place during the first steps of the photocycle of the monomerized form of this retinal protein (Schulenberg et al., 1994). To better understand the origin of the molecular movements observed, we studied the time-resolved volume changes accompanying the photoisomerization of carbocyanines (Churio et al., 1994), polyene dyes that serve as models for photoisomerizable polyene chromophores (e.g., retinal and phytochromobilin) in biological photoreceptors. The molecular volume changes in these cases can be attributed to a volume change of the environment around isomers (the parent state and its photoproduced isomer) of different dipole moment. In other words, from temperature-dependent LIOAS measurements on biological photoreceptors it is possible to follow the time evolution of the chromophore's immediate protein environment.

We decided thus to analyze the photoinduced dynamic behavior of the photoactive yellow protein (PYP) to better understand the nature of the chromophore-protein interactions during

the photoinduced series of transformations in this macromolecule and to extend the thermodynamic description of the PYP photocycle (van Brederode et al., unpublished).

The water soluble PYP (M_r 14 kDa), isolated from various bacteria (Hoff et al., 1994b; Meyer, 1985; Meyer et al., 1990; Van Beeumen et al., 1993) and spectroscopically identified as the pigment controlling negative phototaxis in *Ectothiorhodospira halophila* (Sprenger et al., 1993), has been found to undergo a photoinduced cycle similar to that of the photosensory pigments of halobacteria (Meyer et al., 1987). In the time domain between 2 ns and 2 s, two spectrally distinguishable intermediates have been so far detected (Hoff et al., 1994c; Meyer et al., 1987, 1990). Upon irradiation, the yellow species with an absorption maximum at 446 nm (pG) is bleached in less than 2 ns, and a new species appears with a maximum at 465 nm (pR). Subsequently, this species disappears in ~2 ms and a new absorption is produced at 355 nm (pB). The original yellow color is then recovered again in ~300 ms at room temperature (Hoff et al., 1994c) (see Scheme 1). A global analysis has been applied to a set of

PYP and the transient species formed in subnanosecond times after excitation have overlapping spectra. As a consequence, PYP and the first transient(s) absorb during the exciting pulse, similar to the cases of bacteriorhodopsin (Zimányi and Lanyi, 1993) and other pigments (e.g., phytochrome (Scurlock et al., 1993) and rhodopsin (Lewis and Kliger, 1992)). This consecutive multiphotonic process complicates the determination of the formation quantum yield of the transients by optical methods with relatively long (nanosecond) laser pulses (Rohr et al., 1992).

We report in this paper the determination of the quantum yield for the formation of the red-shifted intermediate pR, i.e., the primary quantum yield by flash photolysis with absorption detection and low exciting photon densities. Temperature-dependent LIOAS measurements afforded the energy content of pR and the accompanying volume change. A kinetic model implying the formation of a photochromic equilibrium, within the laser pulse, between the parent compound and the first transient species was applied to explain the data at relatively high photon densities.

MATERIALS AND METHODS

Protein isolation, purification, and chemicals

PYP was isolated from *E. halophila* according to the published procedure (Hoff et al., 1992; Meyer, 1985; Meyer et al., 1989). The purity of the protein was determined through the ratio of absorbances A_{280}/A_{446}, which was 0.5. For the measurements, PYP was dissolved in 10 mM Tris-HCl (pH 8.0) with 1 mM NaCl. $K_2Cr_2O_7$ and bromcresol purple (Fluka, Neu-Ulm, Germany), each dissolved in the same buffer as PYP, were used as calorimetric references (Braslavsky and Heibel, 1992).

SCHEME 1 Photoinduced transformations of PYP. The lifetimes were obtained by global analysis of various wavelength decays after flash excitation at 25°C. The spectra were derived from global analysis of a set of spectra at various times after flash excitation. (Data from Hoff et al., 1994c.)

Absorption spectroscopy

Absorption measurements were performed with a UV-2102 PC (Shimadzu, Columbia, MD, USA) spectrophotometer. Absorbances were measured to ±0.005 absorbance units.

absorbance decays at various wavelengths, but an unambiguous spectrum to the blue-shifted intermediate could not yet be assigned (Hoff et al., 1994c). Notwithstanding these inherent difficulties, the quantum yield for the photoreaction was reported to be 0.64 from flash photolysis experiments with optical detection (Meyer et al., 1989).

Although the kinetics and spectral shifts of the various transients show similarities to those encountered in other photoreceptors, e.g., in retinal proteins (Mathies et al., 1991; Lewis and Kliger, 1992), the structure of the PYP chromophore has recently been found to be of a new type (Hoff et al., 1994a). In fact, PYP represents a new type of photoreceptor in that it has a thiol ester-linked *p*-coumaric acid as prosthetic group, it is the first photoactive β-clam protein (McRee et al., 1989), and it is the first example of a eubacterial photoreceptor protein, probably involved in a new type of negative phototaxis (Sprenger et al., 1993).

Laser-induced optoacoustic spectroscopy

The LIOAS system has already been described in detail (Braslavsky and Heibel, 1992; Braslavsky and Heihoff, 1989; Churio et al., 1994; Rohr et al., 1992; Schulenberg et al., 1994). The pulse at 308 nm from an Excimer laser (EMG 101 MSG, Lambda Physik, Göttingen, Germany) was used to pump the laser dyes furan 2 (for 408 nm), coumarin 47 (for 458, 460, and 472.5 nm), and coumarin 120 (for 425 and 446 nm) in an FL 2000 dye laser system (Lambda Physik). The resulting pulses had a 10-ns width. The spectrum of the emitted light was confirmed by measurements with an optical multichannel analyzer (OMA III, EG&G). The 10.5-ns pulse from the third harmonic of a Nd:YAG laser (DPLY2, JK Lasers, Rugby, UK) was used for excitation at 355 nm. The piezoelectric detector was a Pb-Zr-Ti ceramic 4-mm diameter and 4-mm thick cylinder (Vernitron) in a homemade housing (Braslavsky and Heihoff, 1989). After amplification, the signal was fed into a Biomation 4500 (Gould, Santa Clara, CA) transient digitizer linked to an LSI 73 (Digital, Maynard, MD) microcomputer connected, in turn, to a VAX main frame. Signal averaging of several traces was performed until a S/N of ~20 was obtained (16–25 traces).

The frequency of excitation of the PYP solutions was always less than 0.2 Hz, allowing a full relaxation of the pigment between pulses (Hoff et al., 1994c). For some experiments at 355 nm this frequency was 1 Hz. No difference was observed between the 1-Hz and the 0.2-Hz experiments.

The LIOAS signal handling has been explained previously in detail (Churio et al., 1994; Malkin et al., 1994). A pinhole of 0.9-mm diameter placed in front of the cuvette limited the acoustic transit time to ~600 ns. The amplitude of the LIOAS signal is proportional to the heat dissipation within this heat integration time (prompt heat) (Braslavsky and Heibel, 1992). The difference between first maximum and first minimum was taken as the signal amplitude (see Figs. 1 and 2).

Convolution of the optoacoustic signal from the reference solution with a model describing the kinetic behavior of the photointermediate produced after excitation of a PYP solution was performed by using a program provided by Dr. C. Viappiani (University of Parma, Parma, Italy) (see Rudzki Small et al., 1991).

Determination of reaction quantum yield by flash photolysis with absorption detection

Flash photolysis with absorption detection and nanosecond excitation was used for the determination of the bleaching recovery quantum yield, as the overlap of the absorption spectra of pR and pG impairs the optical detection of pR formation. The system with photomultiplier detection is similar to the one previously described (Aramendía et al., 1987) with the following changes. The analyzing light was a continuous beam from a Tungsten-halogen lamp attached to a fiber optics illuminator (Oriel 77501). A full account of the changes in the optics that resulted in a much better S/N ratio and permits anisotropy measurements in the transient absorbances, will be published elsewhere (P. Schmidt et al.). The transient recorder was a Tektroniks TDS 520A. The comparative method (Bensasson et al., 1978) was used, with the triplet of tetrasulfonated tetraphenylporphyrin (TPPS) as reference (Davila and Harrimann, 1990; Lambert et al., 1986). The laser system was the same as the one used for LIOAS (vide supra). Excitation was at 408, 425, and 458 nm. Solutions of matched absorbance of TPPS and PYP in the same buffer at either 408 ($A = 0.19$), 425 ($A = 0.15$), or 458 ($A = 0.14$) nm were used. The TPPS solutions were deoxygenated by bubbling N_2 for 10 min. PYP solutions were analyzed under air saturation as this was the condition of the previous studies (Hoff et al., 1994c). Bleaching intensities for PYP at 446 nm and absorbance increases for TPPS at 460 nm were measured 2 ms and 2 μs after excitation, respectively.

RESULTS

Laser-Induced optoacoustic spectroscopy

For the buffer used in our experiments, the LIOAS signal from the calorimetric reference ($K_2Cr_2O_7$) at all wavelengths was indistinguishable from noise at 2.6°C (e.g., see Fig. 1 trace A for $A_{472.5} = 0.12$). At this temperature, a PYP solution showed a strong negative signal (Fig. 1 trace B). This signal had a different polarity from the signal from the same solution at 20°C (Fig. 2). We note that for neat water, the temperature at which the signal from a solution of a calorimetric reference is zero is 3.9°C, i.e., at this temperature the value of the thermal expansion coefficient β for water is zero.

The LIOAS signal was quantitatively treated by using equations already derived (Churio et al., 1994; Malkin et al., 1994; Yruela et al., 1994). Two approaches were used. In one series of experiments, measurements were performed at various temperatures by making use of the strong variation of β with temperature in aqueous solutions (Weast, 1986–1987). The ratio of energy-normalized LIOAS amplitudes for sample (S) and reference (ref) is linearly correlated with the ratio of thermoelastic parameters, $c_p\rho/\beta$

$$\frac{\overline{H^s}}{\overline{H^{ref}}} = \frac{H^S/n^S E_\lambda}{H^{ref}/n^{ref} E_\lambda} = \alpha(\lambda) + \frac{\Phi_R \Delta V_R}{E_\lambda}\left(\frac{c_p\rho}{\beta}\right) \quad (1)$$
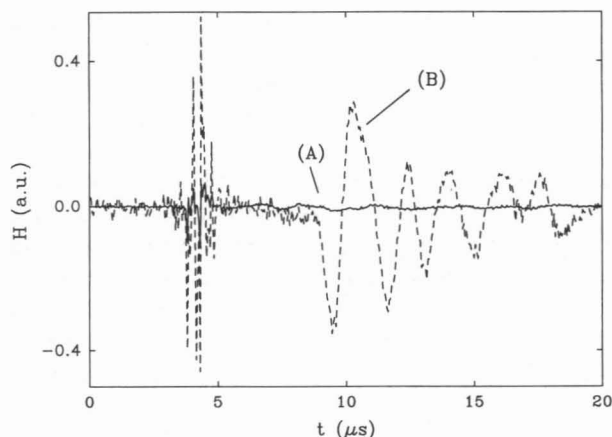

FIGURE 1   Laser-induced optoacoustic signal at 2.6°C from (A) the calorimetric reference solution $K_2Cr_2O_7$ in buffer (see Materials and Methods), in which $\lambda_{exc} = 472.5$ nm and $A_{472.5} = 0.12$; and (B) a PYP solution of the same absorbance.
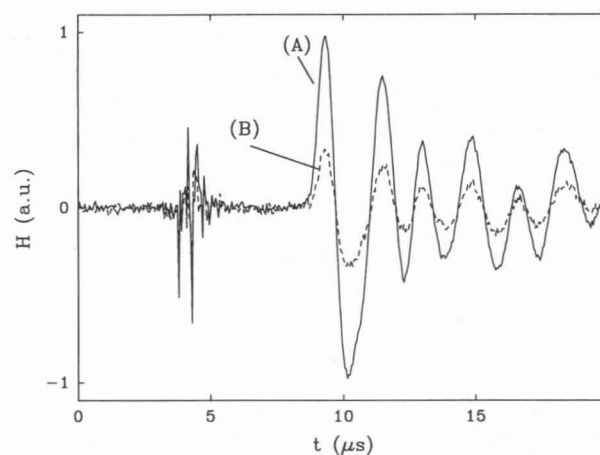

FIGURE 2   Laser-induced optoacoustic signal at 20°C from (A) the calorimetric reference solution $K_2Cr_2O_7$ in buffer (see Materials and Methods), in which $\lambda_{exc} = 472.5$ nm and $A_{472.5} = 0.12$; and (B) a PYP solution of the same absorbance.

where $E_a = n\,E_\lambda$ is the total absorbed energy, i.e., is the number of absorbed Einsteins (n) of energy E_λ, $\alpha(\lambda)$ is the fraction of heat dissipated at each excitation wavelength into the medium within the heat integration time, Φ_R is the reaction quantum yield for the formation of the red-shifted intermediate, c_p is the heat capacity at constant pressure, ρ is the solution mass density, and β is the thermal expansion coefficient. ΔV_R is the specific molar volume change, i.e., the density change induced by the photochemical reaction and integrated over the heat integration time of the experiment (~600 ns). Measurements with PYP solution at all exciting wavelengths showed that at low pulse fluences (<10 μJ per pulse, i.e., small n values) the values of H correlated linearly with the n values. (Some of the data are shown in Figs. 4, 5, and 6). Thus, the slopes of these lines were used in Eq. 1. For the $K_2Cr_2O_7$ and bromcresol purple solutions the energy dependence was linear in the whole energy range used.

Because at 7°C no difference was observed between the energy dependence for the signal from $K_2Cr_2O_7$ in H_2O or in the buffer used, the ratio of thermoelastic parameters in the buffer, $c_p\rho/\beta$, was taken as equal to that in neat H_2O. Should the value of $c_p\rho/\beta$ be different in both media, such a difference would have been more evident at lower than at higher temperatures, as the value of H directly depends on $\beta/c_p\rho$ and the largest differences in the β values occur at temperatures near the zero crossing point. A direct comparison was reported for the case of another buffer by Malkin et al. (1994).

The plot of the left hand side of Eq. 1 versus $c_p\rho/\beta$ for a PYP solution of $A_{460} = 0.23$ and $\lambda_{exc} = 460$ nm is shown in Fig. 3. The value resulting for the volume change per absorbed Einstein is $\Delta V_E = \Phi_R \Delta V_R = -4.8$ ml/Einstein (see Table 1).

The second approach for the determination of the molecular volume change was to measure the amplitudes at two temperatures, i.e., at the temperature for which $\beta = 0$ and the signal is thus due only to molecular volume changes (2.6°C in the buffer used) and at another temperature T for which both the thermal and the molecular volume changes contribute to the pressure wave, i.e., $\beta \neq 0$ (Malkin et al., 1994). Also in this case a measurement with a calorimetric reference at T is needed to calibrate the system. As already shown, Eqs. 2 and 3 describe the handling of the data for this approach (Malkin et al., 1994; Yruela et al., 1994),

$$\alpha = \frac{\overline{H^S}(T_{\beta \neq 0}) - \overline{H^S}(T_{\beta = 0})}{\overline{H^{ref}}(T_{\beta \neq 0})} \qquad (2)$$

$$\Delta V_r = \frac{\overline{H^S}(T_{\beta = 0})}{\overline{H^{ref}}(T_{\beta \neq 0})} \left(\frac{\beta}{c_p\rho}\right)_{T_{\beta \neq 0}} n^S E_\lambda = n^S \Delta V_E. \qquad (3)$$

The top bars indicate that the slopes of the linear parts of the energy-dependent plots of the LIOAS signal amplitudes are used for the calculations.

Fig. 4 shows typical energy dependencies of the LIOAS signal amplitude for the reference and for a PYP solution ($A_{460} = 0.23$) at two temperatures, i.e., at 2.6 ($\beta = 0$) and at

FIGURE 4   Energy dependence of the LIOAS signal amplitude after excitation of a PYP solution with $\lambda_{exc} = 460$ nm and $A_{460} = 0.23$ at ($\triangledown$) 2.6°C, at ($\bigcirc$) 20°C; ($\bullet$) $K_2Cr_2O_7$ solution of the same absorbance and under identical conditions at 20°C.

20°C. Although for the reference solution the dependency was linear in a large energy range, the energy-dependent plots deviated for the PYP solution at both temperatures from linearity already at pulse energies greater than ~10 μJ. This effect will be treated later in the paper (see Fig. 7). As already mentioned, this effect was also found for the other two visible wavelengths studied (472.5 nm with solutions of $A_{472.5} = 0.12$ and 446 nm with solutions of $A_{446} = 0.13$, see Figs. 5 and 6). To increase the accuracy of the results, the experiments with the two-temperature method were repeated as noted in Table 1. For 460 nm, one experiment was carried out at 15°C and two at 20°C. At the other wavelengths, $T_{\beta \neq 0} = 20$°C was always used. In Figs. 4, 5, and 6 only the results from one experiment for each wavelength are plotted.

The slopes of the lines at energies <10 μJ per pulse (0.3 photons per molecule of PYP) were used together with Eqs. 2 and 3 to evaluate the $\alpha(\lambda)$ and ΔV_E values listed in Table 1. The values of the minimal heat dissipated from the lowest excited singlet, i.e., $\alpha_{min} = \alpha(\lambda) - (E_\lambda - E_{0-0})/E_\lambda$, with E_{0-0} being the value of the energy of the 0–0 emission band, are also listed in the Table 1. The value of $E_{0-0} = 255$ kJ/mol was
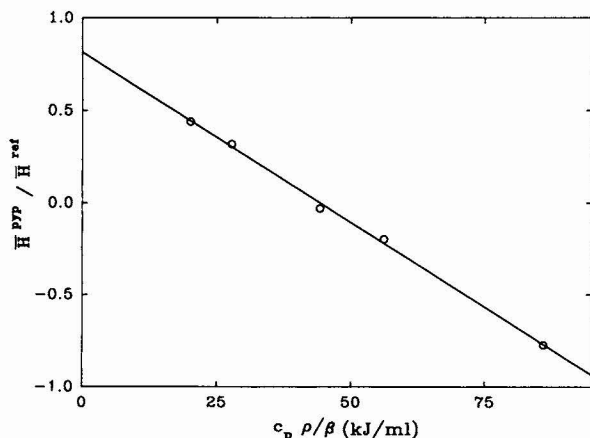

FIGURE 3   Ratio of energy normalized LIOAS signal amplitude for solutions of PYP and $K_2Cr_2O_7$ (as calorimetric reference) as a function of the ratio of thermoelastic parameters $c_p\rho/\beta$. $\lambda_{exc} = 460$ nm; $A_{460} = 0.23$.
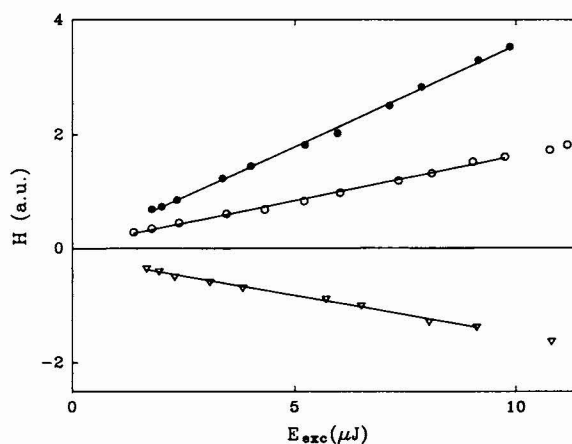
TABLE 1   Volume changes per absorbed Einstein, $\Delta V_E = \Phi_R \Delta V_R$, and fraction of absorbed energy dissipated promptly as heat within 600 ns, $\alpha(\lambda)$, after excitation of a PYP solution at various wavelengths*

λ_{exc} (nm)	ΔV_E (ml/Einstein ± 0.5)	$\alpha(\lambda)$ (± 0.05)	α_{min}	N
460[a]	−4.8	0.81	0.79	–
472.5	−4.7	0.84	0.84	3
460	−5.2	0.85	0.83	3
446	−5.3	0.86	0.81	2
355	−4.0	0.74	0.49	3

* For $\lambda_{exc} = 460$[a] nm, various temperatures and Eq. 1 were used. For the other cases, the two-temperature method was applied with Eqs. 2 and 3 and the number (N) of repeated experiments is indicated (see text). The values of α_{min} at each wavelength were calculated by subtracting from the corresponding $\alpha(\lambda)$ the value $(E_\lambda - E_{0-0})/E_\lambda$ (see text).

obtained from the crossing of the fluorescence excitation and fluorescence emission spectra at 469 nm (Meyer et al., 1991). As expected, within the experimental error, the value of $\alpha_{min} = 0.82 \pm 0.03$ is independent of the excitation wavelength within the blue band. The values for the molecular volume changes are also independent of excitation wavelength $\Delta V_E = -5.0 \pm 0.2$ ml/Einstein.

In Table 1 we also present results for $\lambda_{exc} = 355$ nm. Although the value of ΔV_E is similar to, the value of α_{min} is different from, those at the other wavelengths. However, because after excitation at 355 nm some permanent bleaching of the absorption band was observed (although this was not the case at the other wavelengths), these values were not considered for the calculations.

The results of the convolution for a PYP solution excited at 472.5 nm in the low energy range showed no transient with lifetime in the nano- to microsecond range. The pR transient with its several hundred-microsecond lifetime in the temperature range analyzed, is too long-lived to be resolved by LIOAS. This result demonstrates that no transient with a lifetime longer than a few nanoseconds and shorter than pR stores energy after excitation of PYP.

At laser energies >10 μJ/pulse the amplitudes of the optoacoustic signals from PYP solutions did not follow a linear dependency with the laser energy. Fig. 7 shows the energy dependency for excitation of a PYP solution ($A_{460} = 0.23$) at 460 nm and different temperatures.

Flash photolysis with absorption detection

To calculate the value of the energy content of the first intermediate, as well as the volume change per isomerized molecule, it was necessary to determine the quantum yield of the phototransformation, Φ_R (vide supra). Fig. 8 shows the dependence with the absorbed laser energy (E_a) of the triplet-triplet (T-T) absorption at 460 nm for TPPS 2 μs after excitation and bleaching recovery for PYP at 446 nm 2 ms after

FIGURE 6　Energy dependence of the LIOAS signal amplitude after excitation of a PYP solution with $\lambda_{exc} = 446$ nm and $A_{446} = 0.13$ at ($\triangledown$) 2.6°C and ($\bigcirc$) 20°C; ($\bullet$) $K_2Cr_2O_7$ solution of the same absorbance and under identical conditions at 20°C.

excitation with a laser pulse at 408 nm ([PYP] = 8×10^{-6} M). For the determination of the bleaching-recovery quantum yield of PYP, the slopes of these lines ($\Delta A_{446}/E_a$)$_{PYP}$ and ($\Delta A_{460}/E_a$)$_{TPPS}$ were used together with the absorption coefficient for the TPPS T-T absorption at 460 nm ($\epsilon_{460} = 5.2 \times 10^4$ M^{-1} cm^{-1}), its intersystem crossing quantum yield $\Phi_{TPPS} = 0.60$ (Davila and Harriman, 1990; Lambert et al., 1986), and the absorption coefficient for the solution of PYP at 446 nm (4.5×10^4 M^{-1} cm^{-1}, Meyer, 1985). The value of $\epsilon_{460} = 4.7 \times 10^4$ M^{-1} cm^{-1} for TPPS was obtained by using the comparative method with rose bengal as reference (ϵ_{T-T} at 600 nm = 4.9×10^3 M^{-1} cm^{-1}; $\Phi_T = 0.9$ in phosphate buffer, pH 7) (Gandin et al., 1983). Furthermore, a value of $\epsilon_{460,TPPS} = 5 \times 10^4$ M^{-1} cm^{-1} was derived by using the measured transient absorbance maximum together with the transient species concentration calculated from the volume analyzed by the monitoring beam and the laser fluence. Thus, our $\epsilon_{460,TPPS}$ value agrees with that reported by Lambert et al., 1986 (5.2×10^4 M^{-1} cm^{-1} at 440 nm), and by Bonnet

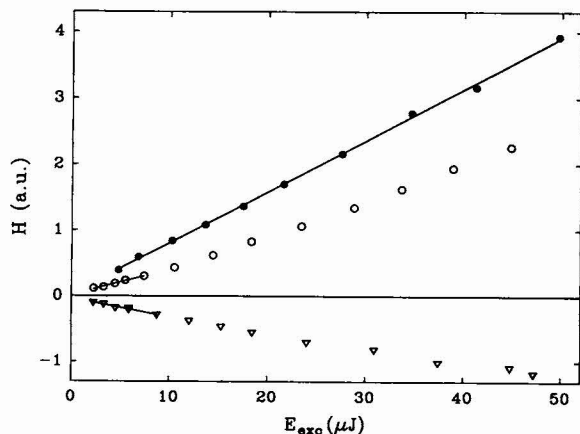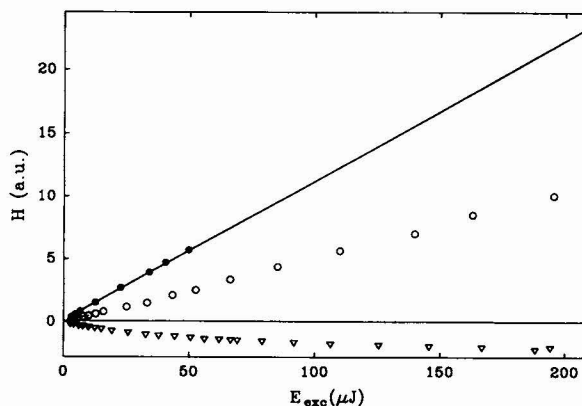

FIGURE 5　Energy dependence of the LIOAS signal amplitude after excitation of a PYP solution with $\lambda_{exc} = 472.5$ nm and $A_{472.5} = 0.11$ at ($\triangledown$) 2.6°C and ($\bigcirc$) 20°C; ($\bullet$) $K_2Cr_2O_7$ solution of the same absorbance and under identical conditions at 20°C.

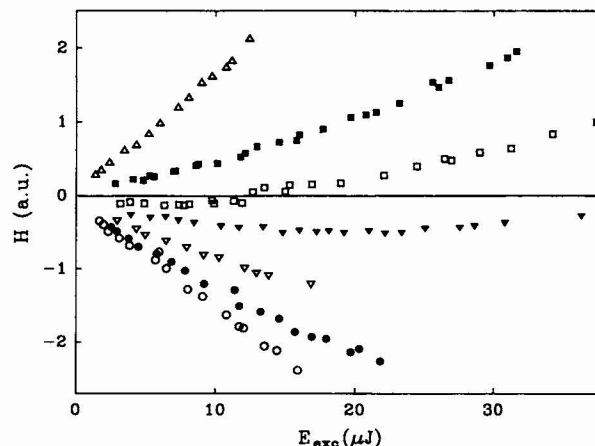FIGURE 7　Laser energy dependence of the LIOAS signal amplitude after excitation of a PYP solution ($A_{460} = 0.23$) with $\lambda_{exc} = 460$ nm at ($\bigcirc$) 2.6, ($\bullet$) 5, ($\triangledown$) 7, ($\blacktriangledown$) 9, ($\square$) 10.5, ($\blacksquare$) 15, and ($\triangle$) 20°C.
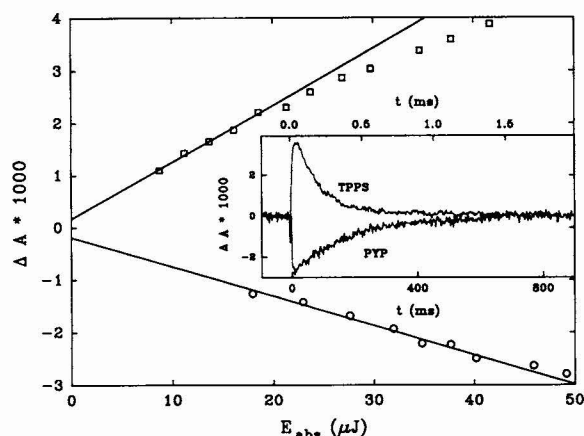
FIGURE 8   Comparative method in flash photolysis. Energy dependence of the amplitude immediately after the laser pulse of the (O) bleaching-recovery of PYP at 446 nm and of the ($\square$) T-T absorption for TPPS at 460 nm for λ_{exc} = 408 nm. The absorbances of the buffer solution (10 mM Tris and 1 mM NaCl, pH 8.0) was A_{408} = 0.19. The inset shows the time evolution of both transient signals.

et al., 1982 (4.5×10^4 M^{-1} cm^{-1} at 460 nm), and it differs significantly from the value reported by Kalyanasundaram and Neumann-Spallart, 1982 (1.3×10^5 M^{-1} cm^{-1} at 460 nm). The bleaching-recovery quantum yield was calculated by the formula

$$\Phi_R = \frac{\Phi_{TPPS}(\Delta A_{446}/E_a)_{PYP}}{(\Delta A_{460}/E_a)_{TPPS}(\epsilon_{460,TPPS}/\epsilon_{446,PYP})}.$$

A value of Φ_R = 0.35 was obtained by using the slope of the lines in Fig. 8. By using similar plots (not shown) for λ_{exc} at 458 nm ([PYP] = 5×10^{-6} M) and 425 nm ([PYP] = 4×10^{-6} M), values of 0.40 and 0.31, respectively, were obtained. The average for the three wavelengths was Φ_R = 0.35 ± 0.05.

DISCUSSION

After excitation (e.g., with a pulse of molar energy E_λ), the PYP chromoprotein molecules may undergo three processes, i.e., they can fluoresce (quantum yield Φ_f and energy maximum E_f), they can store energy in the first intermediate living much longer than the heat integration window of our experiment (600 ns; Φ_R is the reaction quantum yield and E_R the molar energy content), and they can, without radiation, promptly lose their excess energy within the 600 ns (αE_λ is the fraction of absorbed energy promptly lost as heat). Eq. 4 represents the energy balance for the system (see Malkin and Cahen, 1979). As the first intermediate, pR, has a lifetime of several microseconds (Hoff et al., 1994c; Meyer et al., 1987, 1989), and convolution of the LIOAS signal showed no transient shorter than several microseconds, the energy-storing species should be the transient pR

$$E_\lambda = \alpha(\lambda)E_\lambda + \Phi_f E_f + \Phi_R E_R. \qquad (4)$$

It is clear that the values of E_R and of ΔV_R (Eq. 1) strongly

depend on Φ_R. The determination of the latter value and the difficulties arising with the measurements are discussed in the next section.

The reaction quantum yield

Our present value for the quantum yield of the bleaching-recovery of PYP at 446 nm, 0.35 ± 0.05, after excitation with a 10-ns pulse and measured ~2 ms after the pulse, should be identical to the quantum yield of the primary reaction, Φ_R, unless a fast dark branching reaction back to pG occurs in the system, for which there is no indication so far. The competing deactivation processes from excited pG should take place very rapidly, i.e., in a subnanosecond time scale. The measured quantum yield can therefore be taken as identical to Φ_R. Care was taken to use pulse energies as low as possible in the determination of this value to avoid any multiphoton effects. Thus, the data used were only those within the linear energy-dependence region. As high laser energies lead to multiphotonic effects with PYP (see Fig. 9 and the discussion in following paragraphs), as well as with some of the actinometers, the value reported previously, 0.64 (Meyer et al., 1989), may be in error due to these effects. Unfortunately, the authors do not report whether energy-dependent measurements were carried out. It is also possible that errors in this measurement were introduced by the use of erroneous values for the transient molar absorption coefficients of the reference substance. It is well known that molar absorption coefficients of transients are reported with large error margins in the literature and large differences may be encountered depending on the method used for their determination (Bonneau et al., 1991, see also considerations on ϵ of transients in Results).

The energy level of the first PYP photocycle intermediate

Inserting the values Φ_R = 0.35, $\alpha(\lambda)$, and E_λ for excitation within the blue absorption band in the energy balance Eq. 4 (see Table 1) and taking into account that the fluorescence yield of PYP is negligible ($\Phi_f < 2.5 \times 10^{-3}$; Hoff et al., 1992; Meyer et al., 1991), an average value of E_R = E_{pR} = 120 ± 30 kJ/mol is obtained, i.e., ~130 kJ/mol (~50%) lower than the excited PYP molecules (the 0–0 emission band, i.e., the energy level of the first excited singlet state, is at 469 nm $\equiv$ 255 kJ/mol; from Meyer et al., 1991). This is a large energy gap for the primary step. With the reported value of Φ_R = 0.64 (Meyer et al., 1989), a much larger energy gap between PYP and pR would have resulted.

It is worth comparing the results with those obtained with the other biological photoreceptors with polyene chromophores so far studied with time-resolved optoacoustics. In the case of bacteriorhodopsin (BR), we determined an energy content for the intermediate K (with a lifetime of 1.5 μs), of 160 kJ/mol, i.e., 30 kJ/mol (~20%) lower than the excited BR (Rohr et al., 1992). For the case of solubilized rhodopsin, using optoacoustic detection and a relatively large heat integration time, Marr and Peters (1991) determined a very low

energy content (16 ± 24 kJ/mol) for the intermediate(s) present after 1.4 μs of laser excitation, i.e., for lumi-R. In contrast to the PYP system, however, the latter is not the first intermediate for the rhodopsin system (Lewis and Kliger, 1992).

The molecular volume change during the first step of the PYP photocycle

With the value of $\Phi_R = 0.35$ together with the average value for the volume change per absorbed Einstein, $\Delta V_E = -5.0$ ml/Einstein $= \Phi_R \Delta V_R$, a value of $\Delta V_R = -14$ ml/mol is calculated. This is the volume contraction per mol of PYP phototransformed to pR and is equivalent to -24 Å^3 per phototransformed molecule. According to x-ray diffraction data obtained with PYP crystals, the molecule looks like an oblate with axes of 18.5, 16, and 12.5 nm (McRee et al., 1989). With this data a volume of 15,500 Å^3 for the molecule is calculated. Thus, each phototransformed molecule of PYP undergoes a contraction of 0.15% with respect to its volume in the crystal structure. A contraction of 18 Å^3 per phototransformed molecule (11 ml/mol) was determined for the formation of the K isomer from monomeric BR (Rohr et al., 1992). A volume expansion of 29 ml/mol was determined for lumi-R formation from rhodopsin (Marr and Peters, 1991).

Obviously, a contraction is a consequence of a change in density. Thus, it is not sufficient that a reorganization of the molecule takes place since then the van der Waals radii are identical. Rather, dipole moment changes are likely to occur in the chromophore, which in turn induce a reorganization of its immediate environment (protein and/or solvent molecules) around new dipole moments. The reorganization leads then to a contraction. This was the reasoning applied for the case of isomerizable model cyanine dyes in aqueous solution (Churio et al., 1994). In the latter case the contraction was interpreted as a reorientation of water molecules around isomers with different dipole moments. The contraction observed in the case of BR was also attributed to the reorganization of the protein around the photoisomerized intermediate K, with a dipole moment different from BR (Schulenberg et al., 1994).

In the PYP case, the recent determination of the structure of the chromophore as a thioester-linked *p*-coumaric acid (Hoff et al., 1994a) gives rise to the reasonable expectation that, similar to the case of BR (Mathies et al., 1991) and rhodopsin (Lewis and Kliger, 1992), the photochemical primary step is an isomerization of the double bond. As the photoisomer most probably differs from the parent structure with regard to its dipole moment, a rearrangement of the charges of the protein environment could result, leading to the observed contraction.

Modeling of the photochromic system

Compared with the behavior of the calorimetric reference, the nonlinear behavior of the LIOAS signal amplitudes from PYP solutions at relatively high laser energies (see Figs. 4,

5, and 6) indicates that another process takes place in addition to simple excitation of pG and deactivation of pG*. Taking into account the overlap of the absorption spectra of pR and the ground state of PYP (pG) (Meyer et al., 1987; Hoff et al., 1994c) and the fact that the pR state should be created after $\sim$12 ps (Meyer et al., 1991), the back phototransformation of pR to pG within the 10-ns laser pulse is a likely possibility. This type of photochromic equilibrium between the initial form and the first intermediate within the laser pulse duration has been observed in several model systems, e.g., in the laser dye DODCI (Bilmes et al., 1987, 1988) as well as in photoreceptors, like BR (Rohr et al., 1992; Schulenberg et al., 1994) and phytochrome (Braslavsky, 1990; Scurlock et al., 1993; Schaffner et al., 1990). The possibility of a photochromic equilibrium in PYP at room temperature is supported by the low temperature (77 K) experiments that show that pR is photoconverted to pG (Hoff et al., 1992).

We therefore used a four-level model scheme composed of the two ground states, pG and pR, and the corresponding two singlet excited states, pG* and pR*, similar to the case of DODCI (Bilmes et al., 1987, 1988) and BR (Rohr et al., 1992; Schulenberg et al., 1994). Four differential equations describing the time behavior of the four species were used plus a fifth differential equation describing the heat evolution through radiationless processes (the equations are fully described in Bilmes et al., 1987, 1988). All equations were integrated from time $= 0$ up to the acoustic transit time, i.e., 600 ns. The time distribution of the laser pulse was approximated by a Gaussian function. This was experimentally supported by the measurement of the laser-beam profile.

The model served to simulate the energy dependence of the LIOAS signal amplitude at various temperatures and two excitation wavelengths, 446 and 472.5 nm. It was assumed that the pressure originating from the molecular volume change (second term in the right hand side of Eq. 1) was constant with temperature. This is a reasonable assumption, taking into account the small temperature range analyzed. This assumption is supported by the linearity of the plot in Fig. 3. For the energy gap between pG and pR the value determined at low laser energies, namely 120 kJ/mol (vide supra), was used. The lifetime of pR* was assumed identical to that of pG*, i.e., 12 ps (Meyer et al., 1991). There are no data in the literature about the excited state of pR.

In Fig. 9, *C* and *D*, the results of the simulation including (closed symbols) as well as excluding (open symbols) the back phototransformation (pR* $\rightarrow$ pG) are depicted, together with the experimental values in Fig. 9, *A* and *B*. The data in Fig. 9, *A* and *B*, are the same as that shown in Figs. 5 and 6 and, in turn, exhibit a similar behavior as that in Figs. 4 and 8. The experimental data and the simulations shown are for 2.6°C ($\beta = 0$) and 20°C. A value $\Phi_R = 0.35$ (vide supra) was used. For the molar absorption coefficients of pR, we used the values derived by Hoff et al. (1994c) with their kinetic model applied for the interpretation of the time-resolved absorption spectra. These values are ϵ_{446} (pR) $= 1.91 \times 10^4$ and $\epsilon_{472.5}$ (pR) $= 1.96 \times 10^4$ M^{-1} cm^{-1}. The molecular volume change upon back phototransformation
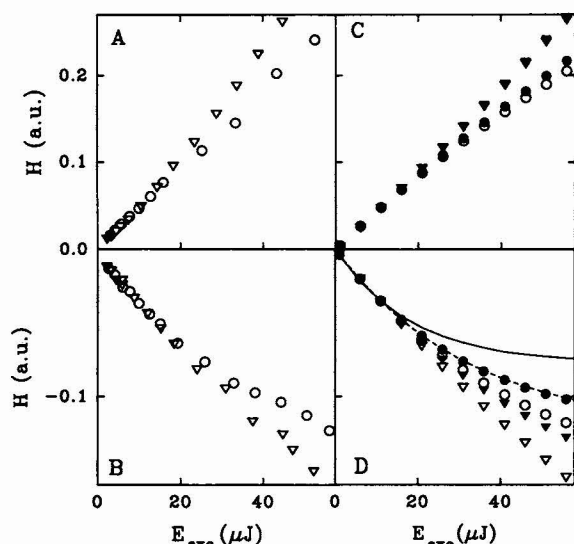
FIGURE 9   Laser energy dependence of the LIOAS signal amplitude after excitation of a PYP solution ($A_{472.5} = 0.11$, 7×10^{-6} M; $A_{446} = 0.13$, 3×10^{-6} M) with (∇) 472.5 and ($\bigcirc$) 446 nm at (A) 20°C and (B) 2.6°C. Simulation of the laser energy dependence of the LIOAS signal amplitude with a four-level model (see text) at 472.5 and 446 nm. Open symbols, without back phototransformation (pR* → pG), and closed symbols, with back phototransformation, at (C) 20°C and (D) 2.6°C. The simulation at 2.6°C, with back phototransformation and $\Phi_R = 0.64$ (Meyer et al., 1989) for (solid line) 446 nm and (dotted line) 472.5 nm is included in D.

from pR to pG should be identical to that for the forward reaction with opposite sign, i.e., an expansion of 14 ml per photoconverted mol.

At both temperatures and at both wavelengths it makes no substantial difference whether the simulation includes or excludes the back phototransformation (pR* → pG). Both simulations mimic the experimental behavior (cf. Fig. 9, D and B). A simple three-level system, with no absorption by pR, would afford a simple saturation curve at 20°C. For each temperature, there is a wavelength-dependent deviation from linearity, which is an obvious consequence of the different absorption coefficients for pR and pG.

Thus, the simulation of our data supports the involvement of a four-level system as a result of multiphotonic absorption. Whether a photochromic equilibrium between pG and pR is established within the 10-ns laser pulse duration cannot be decided with the available set of parameters. A more complete fitting of the model to the experimental data is not possible at the moment as too many parameters are unknown for this system. Furthermore, the expected saturation at 2.6°C could not be experimentally reached at any wavelength due to lack of sufficient energy provided by our laser pulse. Otherwise, a calculation of the quantum yield for the back photoconversion would have been feasible, as in the case with BR (Rohr et al., 1992).

A simulation at both wavelengths and 2.6°C with $\Phi_R = 0.64$ (Meyer et al., 1989) and including back phototransformation with identical quantum yield fits poorly the experimental data (solid and dotted lines in Fig. 9D), i.e., a much

faster deviation of the linear behavior would be expected with such a primary quantum yield.

It is likely that the photochromic equilibrium between pG and pR is reached at relatively high laser energies. It is, however, not realistic to expect that it will be established under natural light conditions in the open field, i.e., the natural habitat for the bacteria. The possibility of multiphotonic processes should certainly play an important role in laboratory measurements on PYP with powerful lasers. Care should be taken to work in these cases in the linear part of the energy dependence.

REFERENCES

Aramendía, P. F., B. P. Ruzsicska, S. E. Braslavsky, and K. Schaffner. 1987. Laser flash photolysis of 124-kilodalton oat phytochrome in H_2O and D_2O solutions: formation and decay of the I_{700} intermediates. *Biochemistry.* 26:1418–1422.

Arata, H., and W. W. Parson. 1981. Enthalpy and volume changes accompanying electron transfer from P-870 to quinones in *Rhodopseudomonas sphaeroides* reaction centers. *Biochim. Biophys. Acta.* 636:70–81.

Bensasson, R., C. R. Goldschmidt, E. J. Land, and T. G. Truscott. 1978. Laser intensity and the comparative method for the determination of triplet quantum yields. *Photochem. Photobiol.* 28:277–281.

Bilmes, G. M., J. O. Tocho, and S. E. Braslavsky. 1987. Laser-induced optoacoustic studies of the photoisomerization of the laser dye 3,3'-diethyloxadicarbocyanine iodide (DODCI). *Chem. Phys. Lett.* 134:335–340.

Bilmes, G. M., J. O. Tocho, and S. E. Braslavsky. 1988. Spectrum, energy content, and relaxation mechanism of the photoisomer of the laser dye 3,3'-diethyloxadicarbocyanine iodide: laser-induced optoacoustic studies. *J. Phys. Chem.* 92:5958–5962.

Bonneau, R., I. Carmichael, and G. L. Hug. 1991. Molar absorption coefficients of transient species in solution. *Pure Appl. Chem.* 63:289–299.

Bonnet, R., R. J. Ridge, E. J. Land, R. S. Sinclair, D. Tait, and T. G. Truscott. 1982. Pulsed irradiation of water-soluble porphyrins. *J. Chem. Soc. Farad. Trans. I.* 78:127–136.

Braslavsky, S. E. 1990. Photochromism in biological systems: phytochrome. *In* Photochromism: Molecules and Systems. H. Dürr and H. Bouas-Laurent, editors. Elsevier, Amsterdam. 738–755.

Braslavsky, S. E., and G. E. Heibel. 1992. Time-resolved photothermal and photoacoustic methods applied to photoinduced processes in solution. *Chem. Rev.* 92:1381–1410.

Braslavsky, S. E., and K. Heihoff. 1989. Photothermal methods. *In* CRC Handbook of Organic Photochemistry I. J. C. Scaiano, editor. CRC Press, Boca Raton, FL. 327–355.

Braslavsky, S. E., A. R. Holzwarth, and K. Schaffner. 1983. Solution conformations, photophysics, and photochemistry of bile pigments; bilirubin and biliverdin dimethyl esters and related linear tetrapyrroles. *Angew. Chem. Int. Ed. Engl.* 22:656–674.

Callis, J. B., W. W. Parson, and M. Gouterman. 1972. Fast changes of enthalpy and volume on flash excitation of *Chromatium* chromatophores. *Biochim. Biophys. Acta.* 267:348–362.

Churio, M. S., K. P. Angermund, and S. E. Braslavsky. 1994. Combination of laser-induced optoacoustic spectroscopy (LIOAS) and semiempirical calculations for the determination of molecular volume changes: the photoisomerization of carbocyanines. *J. Phys. Chem.* 98:1776–1782.

Davila, J., and A. Harriman. 1990. Photoreactions of macrocyclic dyes bound to human serum albumin. *Photochem. Photobiol.* 51:9–19.

Gandin, E., Y. Lion, and A. Van de Vorst. 1983. Quantum yield of singlet oxygen production by xanthene derivatives. *Photochem. Photobiol.* 37:271–278.

Hill, C., W. Gärtner, P. Towner, S. E. Braslavsky, and K. Schaffner. 1994. Expression of phytochrome apoprotein from *Avena sativa* in *Escherichia coli* and formation of photoactive chromoproteins by assembly with phycocyanobilin. *Eur. J. Biochem.* 223:69–77.

Hoff, W. D., P. Düx, K. Hard, B. Devreese, I. M. Nugteren-Roodzant, W. Crielaard, R. Boelens, R. Kaptein, J. Van Beeumen, and K. J. Hellingwerf. 1994a. Thiol ester-linked *p*-coumaric acid as a new photoactive prosthetic group in a protein with rhodopsin-like photochemistry. *Biochemistry.* 33:13959–13962.

Hoff, W. D., S. L. S. Kwa, R. Van Grondelle, and K. J. Hellingwerf. 1992. Low temperature absorbance and fluorescence spectroscopy of the photoactive yellow protein from *Ectothiorhodospira halophila*. *Photochem. Photobiol.* 56:529–539.

Hoff, W. D., W. W. Sprenger, P. W. Postma, T. E. Meyer, M. Veenhuis, T. Lenguijt, and K. J. Hellingwerf. 1994b. The photoactive yellow protein from *Ectothiorhodospira halophila* as studied with a highly specific polyclonal antiserum: (intra)cellular localization, regulation of expression, and taxonomic distribution of cross-reacting proteins. *J. Bacteriol.* 176:3920–3927.

Hoff, W. D., I. H. M. Van Stokkum, H. J. Van Ramesdonk, M. E. Van Brederode, A. M. Brouwer, J. C. Fitch, T. E. Meyer, R. Van Grondelle, and K. J. Hellingwerf. 1994c. Measurement and global analysis of the absorbance changes in the photocycle of the photoactive yellow protein from *Ectothiorhodospira halophila*. *Biophys. J.* 67:1691–1705.

Kalyanasundaram, K., and M. Neumann-Spallart. 1982. Photophysical and redox properties of water-soluble porphyrins in aqueous media. *J. Phys. Chem.* 86:5163–5169.

Lambert, C. R., E. Reddi, J. D. Spikes, M. A. J. Rodgers, and G. Jori. 1986. The effects of porphyrin structure and aggregation state on photosensitized processes in aqueous and micellar media. *Photochem. Photobiol.* 44:595–601.

Lewis, J. W., and D. S. Kliger. 1992. Photointermediates of visual pigments. *J. Bioenergetics Biomembr.* 24:201–210.

Li, L., and J. C. Lagarias. 1992. Phytochrome assembly: defining chromophore structural requirements for covalent attachment and photoreversibility. *J. Biol. Chem.* 267:19204–19210.

Lindemann, P., S. E. Braslavsky, M.-M. Cordonnier, L. H. Pratt, and K. Schaffner. 1993. Effects of bound monoclonal antibodies on the decay of the phototransformation intermediates $I_{700}^{1,2}$ from native *Avena* phytochrome. *Photochem. Photobiol.* 58:417–424.

Malkin, S., and D. Cahen. 1979. Photoacoustic spectroscopy and radiant energy conversion: theory of the effect with special emphasis on photosynthesis. *Photochem. Photobiol.* 29:803–813.

Malkin, S., M. S. Churio, S. Shochat, and S. E. Braslavsky. 1994. Photochemical energy storage and volume changes in the microsecond time range in bacterial photosynthesis: a laser induced optoacoustic study. *J. Photochem. Photobiol. B: Biol.* 23:79–85.

Marr, K., and K. S. Peters. 1991. Photoacoustic calorimetric study of the conversion of rhodopsin and isorhodopsin to lumirhodopsin. *Biochemistry.* 30:1254–1258.

Mathies, R. A., S. W. Lin, J. B. Ames, and W. T. Pollard. 1991. From femtoseconds to biology: mechanism of bacteriorhodopsin's light-driven proton pump. *Annu. Rev. Biophys. Biophys. Chem.* 20:491–518.

McRee, D. E., J. A. Tainer, T. E. Meyer, J. Van Beeumen, M. A. Cusanovich, and E. D. Getzoff. 1989. Crystallographic structure of a photoreceptor protein at 2.4 Å resolution. *Proc. Natl. Acad. Sci. USA.* 86:6533–6537.

Meyer, T. E. 1985. Isolation and characterization of soluble cytochromes, ferredoxins and other chromophoric proteins from the halophilic pho-

totrophic bacterium *Ectothiorhodospira halophila*. *Biochim. Biophys. Acta.* 806:175–183.

Meyer, T. E., J. C. Fitch, R. G. Bartsch, G. Tollin, and M. A. Cusanovich. 1990. Soluble cytochromes and a photoactive yellow protein isolated from the moderately halophilic purple *Rhodospirillum salexigens.* *Biochim. Biophys. Acta.* 1016:364–370.

Meyer, T. E., G. Tollin, T. P. Causgrove, P. Cheng, and R. E. Blankenship. 1991. Picosecond decay kinetics and quantum yield of fluorescence of the photoactive yellow protein from the halophilic purple phototrophic bacterium, *Ectothiorhodospira halophila*. *Biophys. J.* 59:988–991.

Meyer, T. E., G. Tollin, J. H. Hazzard, and M. A. Cusanovich. 1989. Photoactive yellow protein from the purple phototrophic bacterium, *Ectothiorhodospira halophila*. *Biophys. J.* 56:559–564.

Meyer, T. E., E. Yakali, M. A. Cusanovich, and G. Tollin. 1987. Properties of a water-soluble yellow protein isolated from a halophilic phototrophic bacterium that has photochemical activity analogous to sensory rhodopsin. *Biochemistry.* 26:418–423.

Norris, C. L., and K. S. Peters. 1993. A photoacoustic calorimetry study of horse carboxy-myoglobin on the 10-nanosecond time scale. *Biophys. J.* 65:1660–1665.

Ort, D. R., and W. W. Parson. 1978. Flash-induced volume changes of bacteriorhodopsin-containing membrane fragments and their relationship to proton movements and absorbance transients. *J. Biol. Chem.* 253:6158–6164.

Peters, K. S., T. Watson, and T. Logan. 1992. Photoacoustic calorimetry study of human carboxyhemoglobin. *J. Am. Chem. Soc.* 114:4276–4278.

Rohr, M., W. Gärtner, G. Schweitzer, A. R. Holzwarth, and S. E. Braslavsky. 1992. Quantum yields of the photochromic equilibrium between bacteriorhodopsin and its bathointermediate K: femto- and nanosecond optoacoustic spectroscopy. *J. Phys. Chem.* 96:6055–6061.

Rüdiger, W. 1992. Events in the phytochrome molecule after irradiation. *Photochem. Photobiol.* 56:803–809.

Rudzki Small, J., L. J. Libertini, and E. W. Small. 1991. Analysis of photoacoustic waveforms using the nonlinear least squares method. *Biophys. Chem.* 42:29–48.

Schaffner, K., S. E. Braslavsky, and A. R. Holzwarth. 1990. Photochemistry and photophysics of phytochrome. *Adv. Photochem.* 15:229–277.

Schulenberg, P. J., M. Rohr, W. Gärtner, and S. E. Braslavsky. 1994. Photoinduced volume changes associated with the early transformations of bacteriorhodopsin: a laser-induced optoacoustic spectroscopy study. *Biophys. J.* 66:838–843.

Scurlock, R. D., C. H. Evans, S. E. Braslavsky, and K. Schaffner. 1993. A phytochrome phototransformation study using two-laser/two-color flash photolysis: analysis of the decay mechanism of I_{700}. *Photochem. Photobiol.* 58:106–115.

Song, P.-S. 1988. The molecular topography of phytochrome: chromophore and apoprotein. *J. Photochem. Photobiol. B: Biol.* 2:43–57.

Sprenger, W. W., W. D. Hoff, J. P. Armitage, and K. J. Hellingwerf. 1993. The eubacterium *Ectothiorhodospira halophila* is negatively phototactic, with a wavelength dependence that fits the absorption spectrum of the photoactive yellow protein. *J. Bacteriol.* 175:193–215.

Van Beeumen, J. J., B. V. Devreese, S. M. Van Bun, W. D. Hoff, K. J. Hellingwerf, T. E. Meyer, D. E. McRee, and M. A. Cusanovich. 1993. Primary structure of a photoactive yellow protein from the phototrophic bacterium *Ectothiorhodospira halophila*, with evidence for the mass and the binding site of the chromophore. *Protein Science.* 2:1114–1125.

Weast, R. C., editor. 1986–1987. CRC Handbook of Chemistry and Physics, 67th ed. CRC Press, Boca Raton, FL. F4–F5.

Yruela, I., M. S. Churio, T. Gensch, S. E. Braslavsky, and A. R. Holzwarth. 1994. An optoacoustic and singlet oxygen near-IR emission study of the isolated D_1-D_2-cyt b-559 reaction center complex of photosystem II: protein movement associated with charge separation. *J. Phys. Chem.* 98:12789–12795.

Zimányi, L., and J. K. Lanyi. 1993. Deriving the intermediate spectra and photocycle kinetics from time-resolved difference spectra of bacteriorhodopsin: the simpler case of the recombinant D96 N protein. *Biophys. J.* 64:240–251.